Vol 13 No 11, November 2004
1009-1963/2004/13(11)/1951-06

Chinese Physics

© 2004 Chin. Phys. Soc.
and IOP Publishing Ltd

Green's function formalism in semi-infinite composites: an investigation of local field distribution*

Li Chen(李 琛), Gu Ying(古 英)†,
Dai Bing(戴 冰), and Gong Qi-Huang(龚旗煌)‡

State Key Laboratory for Mesoscopic Physics, Department of Physics, Peking University, Beijing 100871, *China*

(Received 27 April 2004; revised manuscript received 9 June 2004)

In the resonant composites, the formerly developed Green's function formalism (GFF) can be used to compute the local field distribution near resonance. In this paper, we extend the GFF in the infinite network to the semi-infinite networks by the method of image. Using the formalism, we investigate the local field distribution near resonance for the impurity clusters with admittance ϵ_0 embedded in one semi-infinite network with ϵ_1. With varying the admittance ϵ_2 of another semi-infinite network, we find that the local fields in the boundary experience great changes, especially at $\epsilon_2 = -\epsilon_1$. The existence of the boundary enhances the localization of the fields within and around the metallic clusters. Therefore, the intensity of local field is influenced by the arrangement of impurity metallic bonds and its distance from the boundary.

Keywords: response to electromagnetic fields, composites
PACC: 7430G, 8160H

1. Introduction

Recently, composite materials have been widely studied. Nanoscale metallic clusters can generate strong non-linear optical responses when they are structured on the dielectric host, through the local-field and geometric resonances.[1,2] Various eigenmode localizations are highly sensitive to the specific local field distribution when resonance takes place.[3−5] Surface-plasmon modes in the disordered nanosystems,[6−8] localized dipolar excitation on the roughly nanostructured surfaces,[9] and selective photomodification in the fractal aggregates of colloidal particles,[10] etc, all directly originate in the local field distribution. Moreover, many experiments have been performed on the composites with impurity metallic clusters embedded in a dielectric host[11] and a large infrared absorption has been observed.[12,13] Meanwhile, the relevant linear and nonlinear optical responses in composite have also been reported to be strongly enhanced due to the giant fluctuations of local fields.[7,14−18]

For a composite material, there exist dielectric resonances due to the positive and negative admittance existing simultaneously. When resonance happens, local electric-fields distribute within or around the impurity clusters. There are very efficient numerical methods to compute the effective conductivity of the composite materials.[19] To avoid the numerical difficulties, the effective-medium theory (EMT)[20] was extended to the nonlinear response of percolating composites and fractal clusters.[21−23] However, for optical nonlinearity, EMT is not an ideal method, which does not allow of the calculations of the fluctuations of local field. EMT is also difficult to deal with composites possessing complex geometric structures. For these reasons, an effective method of Green function formalism (GFF) was developed to compute the local-field distribution in resonant composites.[24,25] In order to investigate the resonant properties to a more generalized extent, in the present paper, we extend the GFF in an infinite network to the semi-infinite

*Project supported by the National Natural Science Foundation of China (Grant Nos 10304001, 10334010, 10328407 and 90101027). The work was also supported by the special fund from Ministry of Science and Technology of China, the National Key Basic Research Special Foundation (Grant No TG1999075207), and the Junzheng Fund.
†E-mail: ygu@pku.edu.cn
‡E-mail: qhgong@pku.edu.cn

network. Then using the formalism, we investigate the local field distribution near resonance for the impurity clusters in the semi-infinite composites.

In the following, the impurity metallic cluster with the admittance ϵ_0 in each bond is embedded in one semi-infinite network with ϵ_1, which is connected with another semi-infinite network with ϵ_2. In the next section, we extend the GFF in an infinite square network to a semi-infinite one by the method of image, then check the correspondence to the Kirchhoff equations in the connecting boundary. Using the GFF, in Section 3, for the impurity cluster, we investigate the local field distribution near resonance in the semi-infinite composites. The numerical calculations are performed to simulate the properties of the local field distribution when the admittance ϵ_2 of the second semi-infinite network is varied from $-\infty$ to $+\infty$ except the value of $\epsilon_2 = -\epsilon_1$. We find that near resonance the local fields at the boundary show sharp changes when $\epsilon_2 \to -\epsilon_1$. Since the existence of the boundary enhances the localization of the fields within and around the metallic clusters, the intensity of local field around the cluster is influenced by the arrangement of the impurity cluster, as well as by its distance from the boundary of two semi-infinite parts. Finally, the main results are summarized in Section 4.

2. Green's function formalism for the semi-infinite composite

In order to develop the GFF in the semi-infinite composite network, we first give the form of the potential of a point charge q in the absence of the impurity clusters in the semi-infinite networks. Consider an infinite square network composed of two semi-infinite parts as shown in Fig.1. When $x > 0$, the admittance in each bond is ϵ_1, while, for $x < 0$, it is ϵ_2. At the boundary, the admittance is set to $\dfrac{\epsilon_1 + \epsilon_2}{2}$.

Now the point charge with q is placed at the position $(x_0,\ y_0)$. Due to the existence of the semi-infinite network $(x < 0)$, the potential F_1 for $x \geq 0$ is looked upon as a superposition of the point charge q at (x_0, y_0) and its image $-\dfrac{\epsilon_2 - \epsilon_1}{\epsilon_1 + \epsilon_2} q$ at $(-x_0, y_0)$. In the following, hold type (such as $\vec{x}$ and $\vec{y}$) will be used to represent vectors. Let $q = 1$, the potential F_1 of a position (x, y) can be denoted as

$$F_1(x,y) = \frac{G(x-x_0, y-y_0)}{\epsilon_1} - \frac{\epsilon_2 - \epsilon_1}{\epsilon_1(\epsilon_2 + \epsilon_1)} \times G(x+x_0, y-y_0), \quad \text{for } x > 0 \qquad (1)$$

while, for $x \leq 0$, the potential F_2 is

$$F_2(x,y) = \frac{2}{\epsilon_1 + \epsilon_2} G(x-x_0, y-y_0), \qquad (2)$$

where F_1 and F_2 are written in terms of the Green function $G_{\vec{x}-\vec{x}_0, \vec{y}-\vec{y}_0}$ of the Laplace operator in the infinite square lattice, i.e. $-\Delta G_{\vec{x},\vec{y}} = \delta_{\vec{x},\vec{y}}$ with $G_{\vec{x},\vec{x}} = 0$. The rationality of $F_1(x,y)$ and $F_2(x,y)$ is examined by checking the correspondence to the Kirchhoff equation inside the network and at the boundary.

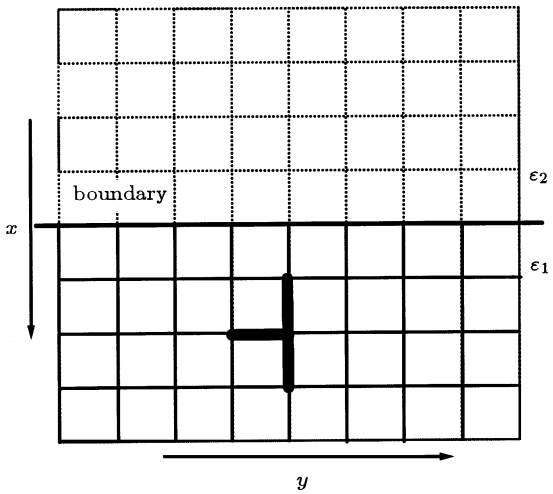


Fig.1. One cluster (shown in thick line) embedded in one of the two connected semi-infinite composites. The upper semi-infinite network has the admittance ϵ_2 in each bond while the lower has ϵ_1.

Then, the GFF in binary composites is reviewed.[5] The impurity metallic clusters with the admittance ϵ_0 in each bond are embedded in an infinite network with the admittance ϵ. The clusters with n impurity metallic bonds constitute the clusters subspace. The subspace is closed and n nontrivial dielectric resonances is determined by the eigenvalues of the Green matrix $\tilde{M}$, written as

$$\tilde{M}_{\vec{x},\vec{y}} = \sum_{\vec{z} \in C(\vec{y})} (G_{\vec{x},\vec{y}} - G_{\vec{y},\vec{z}}), \qquad (3)$$

where $\vec{z} \in C(\vec{y})$ means that the jointing points $\vec{z}$ and $\vec{y}$ belong to the clusters subspace and are the nearest neighbours. $\tilde{M}$ maps the geometric structure of the impurity clusters. The nontrivial eigenvalues of $\tilde{M}$ or dielectric resonances lie in the range $0 \leq s \leq 1$, where $s = 1/(1 - \epsilon_1/\epsilon_0)$. For the mth eigenmode, subject to the point source $(0,0)$, the residues of local field can be written as

$$\text{Residue}(F_{\vec{x},0}) = \frac{1}{\epsilon_0} \left(\sum_{\vec{y} \in C} \tilde{L}_{m,\vec{y}} \tilde{G}_{\vec{y},0} \right) \times \sum_{\vec{z} \in C} M_{\vec{x},\vec{z}} \tilde{R}_{m,\vec{z}}, \qquad (4)$$

where $\tilde{R}_m$ and $\tilde{L}_m$ are the mth right and left eigenvectors of Green matrix $\tilde{M}$, $\tilde{G}_{\vec{y},0}$ is the Green function of the site $\vec{y}$ within the clusters subspace subject to the point source $(0,0)$, and $M_{\vec{x},\vec{z}} = \sum_{\vec{y}\in C(\vec{z})} (G_{\vec{x},\vec{z}} - G_{\vec{x},\vec{y}})$. By introducing the difference admittance ratio[25] $\eta = (\epsilon_2 - \epsilon_0)/(\epsilon_1 - \epsilon_0)$, the GFF is extended to three-component composites. Moreover, by calculating the values of the Green function in 3D, the GFF can be extended to 3D.

Now the impurity metallic cluster with the admittance ϵ is added into the semi-infinite networks with the admittance ϵ_1 and ϵ_2, as shown in Fig.1. The values of dielectric resonances should not be changed since the influence of the infinite semi-infinite network is infinitely small. The electrostatic Green function in the two semi-infinite networks can be worked out by the method of image. The point source is placed at $\vec{x}_0$. For $x \geq 0$, the electrostatic potential H_1 at $\vec{x}$ can be written as

$$\begin{aligned} H_1(\vec{x},\vec{x}_0) =& F_1(\vec{x},\vec{x}_0) + \sum_{n=1}^{n_R} \frac{1}{(s-s_n)\epsilon_1} \\ & \times \left(\sum_{\vec{y}\in C} \tilde{L}_{n,\vec{y}} \tilde{G}_{\vec{y},\vec{x}_0} \right) \\ & \times \left[\sum_{\vec{z}\in C} \tilde{M}_{\vec{x},\vec{z}} \tilde{R}_{n,\vec{z}} - \left(\frac{\epsilon_2 - \epsilon_1}{\epsilon_2 + \epsilon_1} \right) \right. \\ & \left. \times \sum_{\vec{z}'\in C'} \tilde{M}_{\vec{x},\vec{z}'} \tilde{R}_{n,\vec{z}'} \right] \end{aligned} \tag{5}$$

with

$$\begin{aligned} F_1(\vec{x},\vec{y}) =& \frac{G(x-x_0, y-y_0)}{\epsilon_1} \\ & - \frac{\epsilon_2 - \epsilon_1}{\epsilon_1(\epsilon_2+\epsilon_1)} G(x+x_0, y-y_0), \end{aligned} \tag{6}$$

while, for $x \leq 0$, the potential H_2 is written as

$$\begin{aligned} H_2(\vec{x},\vec{x}_0) =& F_2(\vec{x},\vec{x}_0) + \sum_{n=1}^{n_R} \frac{1}{(s-s_n)\epsilon_2} \\ & \times \left(\sum_{\vec{y}\in C} \tilde{L}_{n,\vec{y}} \tilde{G}_{\vec{y},\vec{x}_0} \right) \\ & \times \left[\left(\frac{2\epsilon_2}{\epsilon_2+\epsilon_1} \right) \sum_{\vec{z}\in C} \tilde{M}_{\vec{x},\vec{z}} \tilde{R}_{n,\vec{z}} \right] \end{aligned} \tag{7}$$

with

$$F_2(\vec{x},\vec{y}) = \frac{2}{\epsilon_1+\epsilon_2} G(x-x_0, y-y_0), \tag{8}$$

where C' is the image of C, that is to say, when C is localized at (x,y), the location of C' is $(-x,y)$. At the boundary, the admittance must be set to $(\epsilon_1+\epsilon_2)/2$. The electric potentials diverge and localize around the clusters when s is close to one of the eigenvalues. Only those nontrivial eigenvalues ($s \neq 0$, or 1) correspond to the real physical resonances.

We will check the correspondence of $H_1(\vec{x},\vec{x}_0)$ and $H_2(\vec{x},\vec{x}_0)$ to the Kirchhoff equations, especially at the boundary of the two semi-infinite networks. As shown in Fig. 2, $\vec{0}(0,y)$ is an arbitrary point at the boundary. The four nearest neighbours of the point $\vec{0}(0,y)$ are marked as $\vec{1}(0,y-1)$, $\vec{2}(0,y+1)$, $\vec{3}(-1,y)$ and $\vec{4}(1,y)$, as shown in Fig. 2. The continuity of potential at the point $\vec{0}(0,y)$ is proved, i.e. $H_1(\vec{0},\vec{x}_0) = H_2(\vec{0},\vec{x}_0) = H_0(\vec{0},\vec{x}_0)$. Therefore, the potentials at $\vec{1}$ and $\vec{2}$ have the form

$$\begin{aligned} H_0(\vec{1},\vec{x}_0) =& F_0(\vec{1}) + \sum_{n=1}^{n_R} \frac{2}{(s-s_n)(\epsilon_1+\epsilon_2)} \\ & \times \sum_{\vec{y}\in C} \tilde{L}_{n,\vec{y}} \tilde{G}_{\vec{y},\vec{x}_0} \sum_{\vec{z}\in C} \tilde{M}_{\vec{1},\vec{z}} \tilde{R}_{n,\vec{z}}, \end{aligned} \tag{9}$$

and

$$\begin{aligned} H_0(\vec{2},\vec{x}_0) =& F_0(\vec{2}) + \sum_{n=1}^{n_R} \frac{2}{(s-s_n)(\epsilon_1+\epsilon_2)} \\ & \times \sum_{\vec{y}\in C} \tilde{L}_{n,\vec{y}} \tilde{G}_{\vec{y},\vec{x}_0} \sum_{\vec{z}\in C} \tilde{M}_{\vec{2},\vec{z}} \tilde{R}_{n,\vec{z}}. \end{aligned} \tag{10}$$

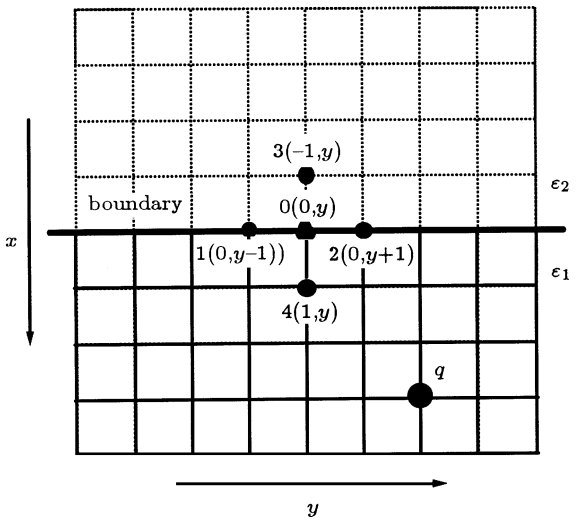


Fig.2. Points $\vec{0},\vec{1},\vec{2}$ are on the boundary, while points $\vec{3}$, $\vec{4}$ are above and below the point $\vec{0}(0,y)$, respectively.

Then we consider the potentials in the direction x. The form of the Green function can be written as

$$\begin{aligned} H_1(\vec{3},\vec{x}_0) =& F_1 + \sum_{n=1}^{n_R} \frac{1}{(s-s_n)\epsilon_1} \left(\sum_{\vec{y}\in C} \tilde{L}_{n,\vec{y}} \tilde{G}_{\vec{y},\vec{x}_0} \right) \\ & \times \left[\sum_{\vec{z}\in C} \tilde{M}_{\vec{x},\vec{z}} \tilde{R}_{n,\vec{z}} - \left(\frac{\epsilon_2 - \epsilon_1}{\epsilon_2 + \epsilon_1} \right) \right. \\ & \left. \times \sum_{\vec{y}'\in C'} \tilde{M}_{\vec{x},\vec{z}'} \tilde{R}_{n,\vec{z}'} \right], \end{aligned} \tag{11}$$

with

$$F_1 = \frac{G(1-x_0, y-y_0)}{\epsilon_1} - \frac{\epsilon_2-\epsilon_1}{\epsilon_1(\epsilon_2+\epsilon_1)} G(1+x_0, y-y_0), \qquad (12)$$

and

$$H_2(\vec{4},\vec{x}_0) = F_2 + \sum_{n=1}^{n_R} \frac{1}{(s-s_n)\epsilon_2} \Big(\sum_{\vec{y}\in C} \tilde{L}_{n,\vec{y}} \tilde{G}_{\vec{y},\vec{x}_0} \Big) \times \Big[\Big(\frac{2\epsilon_2}{\epsilon_2+\epsilon_1} \Big) \sum_{\vec{y}\in C} \tilde{M}_{\vec{x},\vec{z}} \tilde{R}_{n,\vec{z}} \Big], \qquad (13)$$

with

$$F_2 = \frac{2}{\epsilon_1+\epsilon_2} G(1+x_0, y-y_0). \qquad (14)$$

For simplicity, the unit point source is placed at $\vec{0}(0,0)$. For an arbitrary point $\vec{0}(0,y)$ (other than the point $\vec{0}(0,0)$), the electric potential should satisfy the Kirchhoff equation

$$\sum_{y(\vec{x})} \epsilon_{\vec{x},\vec{y}} (H_{\vec{x},0} - H_{\vec{y},0}) = 0. \qquad (15)$$

Substituting Eqs.(9), (10), (11), and (13) into the Kirchhoff Eq.(15), we have the following form:

$$\frac{\epsilon_1+\epsilon_2}{2}[H_0(\vec{1},\vec{x}_0) + H_0(\vec{2},\vec{x}_0) - 2H_0(\vec{0},\vec{x}_0)] + \epsilon_1[H_1(\vec{3},\vec{x}_0) - H_0(\vec{0},\vec{x}_0)] + \epsilon_2[H_2(\vec{4},\vec{x}_0) - H_0(\vec{0},\vec{x}_0)] = 0. \qquad (16)$$

Thus we have obtained the Green function formalism for the semi-infinite composites. In the next section, we use the GFF to investigate the local field distribution near resonances in the semi-infinite composites.

3. Local-field distribution near resonance

In the infinite binary composites, local field distribution has been widely studied.[1,3,5,24,26,27] Near resonance, the existence of another semi-infinite network will influence the local field. In this section, one-bond metallic cluster is used to represent the impurity cluster. A single bond with the admittance ϵ embedded in one semi-infinite network with $\epsilon_1(=1.0)$ is parallel to the boundary. The local fields near resonance within

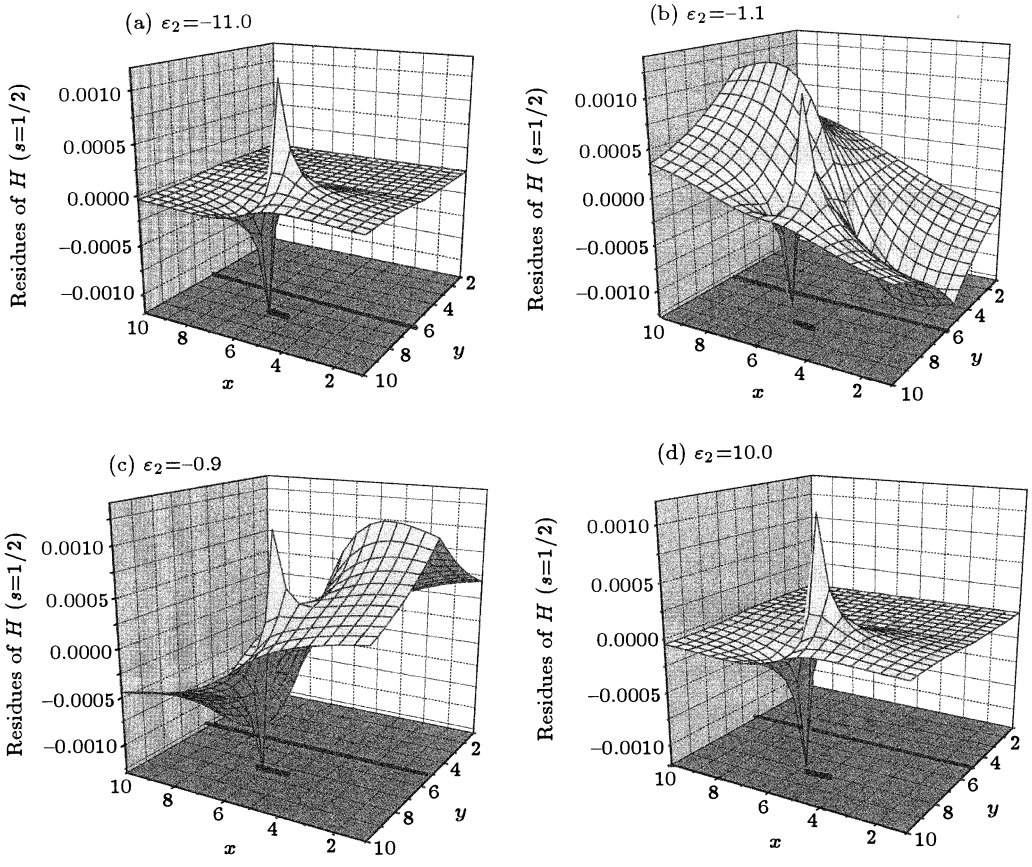


Fig.3. 3D plots of the residues of potential of one bond embedded in the two connected semi-infinite networks. The bond is shown as a thick bar while the source is located at $(0,0)$. Here $\epsilon_1 = 1.0$. (a) $\epsilon_2 = -11.0$, (b) $\epsilon_2 = -1.1$, (c) $\epsilon_2 = -0.9$, and (d) $\epsilon_2 = 10.0$.

or around the clusters are shown in Fig.3 with varying the admittance ϵ_2 of the other semi-infinite network in a wide range. We obtain the similar result to what was found in the infinite binary composite,[24] i.e. the field is very localized near resonance. When $|\epsilon_2 - \epsilon_1| >> \epsilon_1$, another semi-infinite network with ϵ_2 has no obvious effect on the local field, as shown in Fig.3(a) with $\epsilon_2 = -11.0$ and in Fig.3(d) with $\epsilon_2 = 10.0$. For $\epsilon_2 = -\epsilon_1$, there is a divergence in the local field at the boundary. We think that this divergence has not an obvious physical meaning. However, when $\epsilon_2 \to -\epsilon_1$ from both sides, we find that the local fields at the boundary have symmetric changes, as shown in Fig.3(b) with $\epsilon_2 = -1.1$ and in Fig.3(c) with $\epsilon_2 = -0.9$. From Figs.3(a), (b), (c) and (d), we find that the intensity of local field has no obvious change with the increment of the admittance ϵ_2. The results are depicted in Fig.4 by a 2D plot. In Fig.4, we also find that when $\epsilon_2 = -11.0$ and $\epsilon_2 = 10.0$, the curves of local fields almost overlap the curve for $\epsilon_2 = \epsilon_1 = 1.0$.[24] Due to the influence of the other semi-infinite network, for $\epsilon_2 = -1.1$, the field is more localized, while for $\epsilon_2 = -0.9$, the field becomes more extended. Furthermore, the numerical results also indicate that the residues of electric potentials have the similar tendency described above for two- or multi-bond metallic clusters.

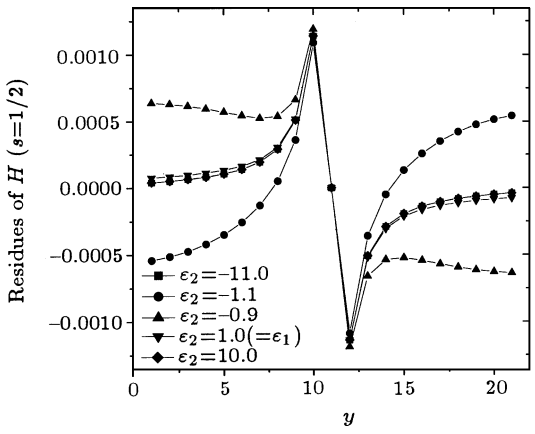


Fig.4. 2D plots of the residues of potential of one bond embedded in the two connected semi-infinite networks. The same parameters are set as in Fig.3. The admittance ϵ_2 is set respectively as -11.0, -1.1, -0.9, 1.0 and 10.0, shown by different symbols.

Then, we investigate the local field distribution of eigenmode for different arrangement of the one-bond cluster. This can be used to represent a multi-bond cluster. Similar to Fig.1, here the boundary is set at $x = 10$ with the admittance $\frac{\epsilon_1 + \epsilon_2}{2}$. For $x > 10$, $\epsilon_1 = 1.0$ and for $x < 10$, $\epsilon_2 = -3.0$. In the parallel case, the bond is located from $(16, 10)$ to $(16, 11)$, while in the vertical case, the bond is located from $(15, 10)$ to $(16, 10)$. As depicted in Fig.5, the curve with square symbols show the local fields near resonance for the parallel case, while the curve with circle symbols the vertical case. We observe that for both cases the fields are localized within and around the metallic clusters. However, the boundary causes the enhancement of the local field. The vertical bond is closer in distance than the parallel bond. Therefore, in the vertical case, the intensity of fields is greater.

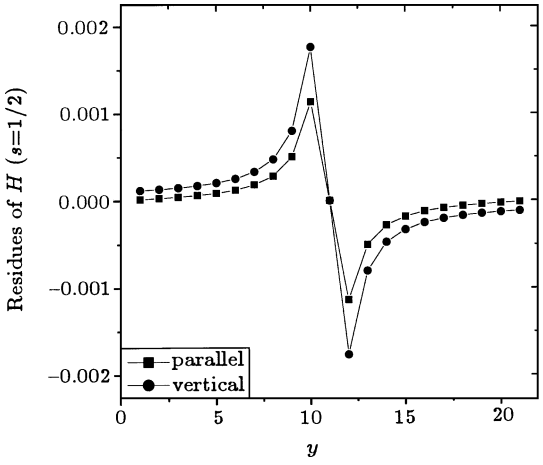


Fig.5. 2D plot of the residues of potential of one parallel or vertical bond. $\varepsilon_1 = 1.0$ and $\varepsilon_2 = -3.0$. The source is located at $(0, 0)$ and the boundary at $x = 10$. For the parallel case, the bond is located from $(16, 10)$ to $(16, 11)$, while for the vertical case, the bond is from $(15, 10)$ to $(16, 10)$.

In order to see the boundary effect more clearly, we investigate the local field near resonance when the bond is close to or far from the boundary. The boundary is still set as $x = 10$. As defined in Fig.5, $\epsilon_1 = 1.0$ and $\epsilon_2 = -3.0$. When the bond is located from $(16, 10)$ to $(16, 11)$, i.e. far from the boundary, its distance is $d = 6$, while for the bond located from $(14, 10)$ to $(14, 11)$, i.e. close to the boundary, $d = 4$. The local fields near resonance are shown as the curve with square symbols for $d = 6$ and the curve with circle symbols for $d = 4$ in Fig.6. From the figure, we see clearly that the fields are more localized when the bond is closer to the boundary. Therefore, we conclude that the existence of the boundary enhances the localization of the field.

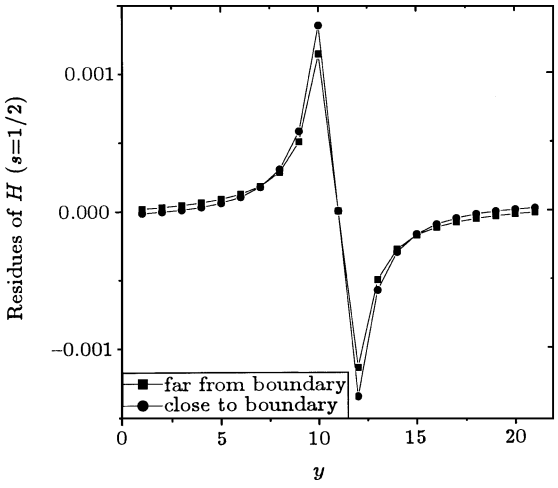


Fig.6. 2D plot of the residues of potential of one bond close to and far from the boundary. $\varepsilon_1 = 1.0$ and $\varepsilon_2 = -3.0$. The source is located at $(0, 0)$ and for the boundary at $x = 10$. Far from the boundary, the bond is located from $(16, 10)$ to $(16, 11)$ or $d = 6$. Close to the boundary, the bond is from $(14, 10)$ to $(14, 11)$ or $d = 4$.

5. Summary

In summary, we have extended the GFF in the infinite network to the semi-infinite networks by the method of image. Using the formalism, we investigated the local field distribution near resonance for the impurity clusters with admittance ϵ_0 embedded in one semi-infinite network with ϵ_1. With varying the admittance ϵ_2 of the other semi-infinite network, the local fields in the boundary experience great changes, especially at $\epsilon_2 = -\epsilon_1$. However, when resonance happens, the field is still localized within and around the clusters. Further numerical calculations also indicate that the existence of the boundary enhances the localization of the fields. Therefore, the intensity of local field is influenced by the arrangement of impurity metallic bonds and its distance from the boundary. The local field distribution is useful for understanding further the optical properties of metal–dielectric composites.

Acknowledgements

We acknowledge useful discussions with Professor Zhao K H.

References

[1] Shalaev V M 1996 *Phys. Rep.* **272** 61
[2] Clerc J P, Giraud G, Luck J M and Robin Th 1996 *J. Phys.* A **29** 4781
[3] Stockman M I 2000 *Phys. Rev.* B **62** 494
[4] Stockman M I 1997 *Phys. Rev.* E **56** 6494
[5] Gu Y, Yu K W and Yang Z R 2002 *Phys. Rev.* B **66** 012202
[6] Markel V A, Shalaev V M, Zhang P, Huynh W, Tay L, Haslett T L and Moskovits M 1999 *Phys. Rev.* B **59** 10 903
[7] Sarychev A K, Shubin V A and Shalaev V M 1999 *Phys. Rev.* B **60** 16 389
[8] Stockman M I, Faleev S V and Bergman D J 2001 *Phys. Rev. Lett.* **87** 167401
[9] Bozhevolnyi S I, Markel V A, Coello V, Kim W and Shalaev V M 1998 *Phys. Rev.* B **58** 11 441
[10] Safonov V P, Shalaev V M, Markel V A, Danilova Y E, Lepeshkin N N, Kim W, Rautian S G and Armstrong R L 1998 *Phys. Rev. Lett.* **80** 1102
[11] Devaty R P and Sievers A J 1984 *Phys. Rev. Lett.* **52** 1344
[12] Tanner D B, Sievers A J and Buhrman R A 1975 *Phys. Rev.* B **11** 1330
[13] Granqvist C G, Buhrman R A, Wyns J and Sievers A J 1976 *Phys. Rev. Lett.* **37** 625
[14] Stockman M I 2000 *Phys. Rev. Lett.* **84** 1011
[15] Gadenne M, Podolskiy V, Gadenne P *et al.* 2001 *Europhys. Lett.* **53** 364
[16] Shalaev V M and Sarychev A K 1998 *Phys. Rev.* B **57** 13265
[17] Gu Y and Yu K W 2002 *Chin. Phys.* **11** 601
[18] Wei E B, Tian J W and Song J B 2004 *Chin. Phys.* **13** 388
[19] For a review, see Bergman D J and Stroud D 1992 *Solid State Physics* edited by Ehrenreich H and Turnbull D (New York: Academic) **146** p147
[20] Kirkpatrick S 1973 *Rev. Mod. Phys.* **45** 574
[21] Stroud D and Hui P M 1998 *Phys. Rev.* B **37** 8719
[22] Zeng X C, Hui P M, Bergman D J and Stroud D 1989 *Phys. Rev.* B **39** 13224
[23] Yuen K P, Law M F, Yu K W and Sheng P 1997 *Phys. Rev.* E **56** 1322
[24] Gu Y, Yu K W and Sun Hong 1999 *Phys. Rev.* B **59** 12847
[25] Gu Y and Gong Q H 2003 *Phys. Rev.* B **67** 014209
[26] Gu Y and Gong Q H 2002 *J. Phys.: Condens. Matter* **14** 6567
[27] Gu Y, Yu K W and Yang Z R 2002 *Phys. Rev.* E **65** 046129